

# Mechanism of superconductivity in $K_3C_{60}$

(alkali/Buckminsterfullerene/electron–phonon coupling)

GUANHUA CHEN AND WILLIAM A. GODDARD III

Materials and Molecular Simulation Center, California Institute of Technology, 139-74, Pasadena, CA 91125

Contributed by William A. Goddard III, November 13, 1992

**ABSTRACT** Using electronic states and phonon states from the first-principles calculations and including both conventional electron–phonon charge coupling and Jahn–Teller coupling, we predict  $T_c$  and other superconducting properties. The only adjustable parameter in the theory is the screening length,  $R_{sc}$ . Using  $R_{sc} = 0.8$ – $1.0$  Å, we find excellent agreement with experiment for  $T_c$  (16–18 K), pressure dependence of  $T_c$  ( $\Delta T_c = -6$  to  $-10$  K for 1 GPa), and  $^{12}C$  to  $^{13}C$  isotope shift ( $\alpha_C = 0.2$ ); experimental values: 19 K,  $-7$  K, and 0.3, respectively.

A number of superconducting alkali compounds of  $C_{60}$  ( $M_3C_{60}$ ) have been synthesized (1–5), leading to transition temperatures  $T_c$  from 2.5 K to 33 K. Several quite different mechanisms (6–12) have been proposed to explain the superconductivity in these materials.

A suggestion by Lannoo *et al.* (6, 7), Johnson *et al.* (8) and Varma *et al.* (9) is that dynamic Jahn–Teller (JT) coupling involving high-frequency intramolecular vibrations strongly scatter electrons near the Fermi surface, leading to superconductivity. On the other hand, Zhang *et al.* (10) estimated various contributions to the electron–electron interaction in  $K_3C_{60}$  and argued that the  $K^+$  optical–phonon modes induce a strong attraction that is the main source of superconductivity. In addition to phonon-mediated electron–pairing mechanisms, Chakravarty *et al.* (11) and Baskaran and Tosatti (12) argue that two electrons may pair by electron–electron exchange and correlation on a single  $C_{60}$  molecule.

## Hamiltonian and Electron–Phonon Couplings

We present here a first-principles, quantitative study of the superconductivity  $K_3C_{60}$ , using the Hamiltonian equation

$$H = H_{ph} + H_e + H_{ee} + H_{eph}^Q + H_{eph}^{JT}, \quad [1]$$

where each term is defined below.

**Phonon States ( $H_{ph}$ ).** We started with the graphite force field (GraFF) developed by Guo *et al.* (13) for describing the structure, elastic constants, and phonons of graphite and intercalated graphite. Without adjustments, the GraFF leads to an excellent description of the vibrational levels of  $C_{60}$  (4% average absolute error for  $A_g$  and  $H_g$ ). The lattice constants of  $K_3C_{60}$  are within 0.1 Å of experiment (14, 15), and the predicted linear compressibilities (13) of  $K_3C_{60}$ ,  $\beta = 1.13 \times 10^{-3}$  kbar $^{-1}$ , is close to experiment (15),  $1.20(9) \times 10^{-3}$  kbar $^{-1}$ .

Using the predicted structure of fcc  $K_3C_{60}$  [ $a = 14.18$  Å, experimental (14, 15)  $a = 14.24$  Å], we calculated the 189 phonon modes (eigenvectors and frequencies) for each point of a  $6 \times 6 \times 6$  grid in the Brillouin zone. These modes partition into 174 high-frequency intramolecular bands (260–1520  $cm^{-1}$ ) plus six lattice modes (130–140  $cm^{-1}$ ) involving

tetrahedral K, three lattice modes (20–50  $cm^{-1}$ ) involving octahedral K, three  $C_{60}$  librational modes (30–40  $cm^{-1}$ ), and three acoustic phonon modes. We write  $H_{ph}$  as

$$H_{ph} = \sum_{k,j} \Omega_{kj} a_{kj}^+ a_{kj}, \quad [2]$$

where  $\Omega_{kj}$  is the frequency of mode  $j$  ( $j = 1189$ ) with momentum  $k$ .

**Electronic States ( $H_e$ ).** For  $H_e$  we fitted the local density approximation (LDA) description of the conduction band by Erwin and Pickett (16) to a tight-binding Hamiltonian

$$H_e = \sum_{i,j} t_{ij}^{(1)} c_{mi}^+ c_{nj} + \sum_k t_k^{(2)} c_{mk}^+ c_{lk}, \quad [3]$$

with the nearest ( $nn$ ) and the next-nearest neighbor ( $nnn$ ) hopping matrix elements. This leads to a density of states of  $N(0) = 11.5$  [the units of  $N(0)$  are states per eV per  $C_{60}$ ] and a Fermi energy of  $E_f = 0.23$  eV. These compare well with the LDA results (16) of  $N(0) = 13.2$  and  $E_f = 0.26$  eV.

We determined the Fermi surface by calculating the states from  $H_e$  at 1,000,000 points in the Brillouin zone, evaluating the Fermi energy, and selecting 330 points within 0.001 eV of the Fermi energy.

**Dynamic Charge Coupling ( $H_{eph}^Q$ ).** Dynamic charge coupling describes the changes in the electron–ion coulomb interactions, due to vibrations (for fixed electronic orbitals). We calculated the electron–phonon coupling matrix  $M_{k'kj}$ , using the exact phonon eigenvectors and eigenenergies with a local Wannier orbital representation for the conduction electrons.

The charge-coupling Hamiltonian is written as

$$H_{eph}^Q = \sum_l \sum_{n\alpha} \Delta \mathbf{R}_{n\alpha} \cdot \nabla_{n\alpha} V_{ei}(\mathbf{r}_l - \mathbf{R}_{n\alpha}^{(0)}), \quad [4]$$

where  $V_{ei}(r) = \exp(-r/R_{sc})/r$  is the screened electron–ion coulomb interaction with screening length  $R_{sc}$ ,  $\mathbf{R}_{n\alpha}^{(0)}$  is the equilibrium position of the  $\alpha$ th ion in the  $n$ th unit cell, and  $\Delta \mathbf{R}_{n\alpha}$  is its displacement,

$$\Delta \mathbf{R}_{n\alpha} = \sum_{k,j} \sqrt{1/NM_\alpha} Q(k,j) \xi(\alpha|k,j) \exp(i\mathbf{k} \cdot \mathbf{R}_{n\alpha}^{(0)}), \quad [5]$$

where  $\xi(\alpha|k,j)$  is the phonon eigenvector of momentum  $k$  and mode  $j$  and  $Q(k,j)$  is its amplitude.

Using the tight-binding picture,  $H_{eph}^Q$  simplifies to

$$H_{eph}^Q = \frac{1}{V^{1/2}} \sum_{k'kj} M_{k'kj} c_{k'}^+ c_k (a_{-qj}^+ + a_{qj}) \quad [6]$$

$$M_{k'kj} = -i \sum_{G,\alpha} \left( \frac{\hbar}{2\rho_\alpha \Omega_{qj}} \right)^{1/2} e^{-i\mathbf{G} \cdot \mathbf{R}_\alpha} \hat{V}_{ei}(\mathbf{q} + \mathbf{G}) \xi(\alpha|q,j) \cdot (\mathbf{q} + \mathbf{G}) W(\mathbf{q} + \mathbf{G}; \mathbf{k}', \mathbf{k}), \quad [7]$$

The publication costs of this article were defrayed in part by page charge payment. This article must therefore be hereby marked "advertisement" in accordance with 18 U.S.C. §1734 solely to indicate this fact.

Abbreviations: LDA, local density approximation; JT, Jahn–Teller.

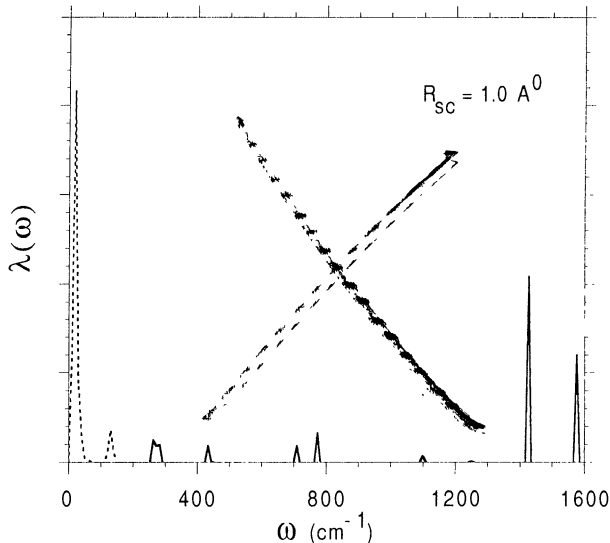


FIG. 1. Calculated values of  $\lambda(\omega) = 2\alpha^2(\omega)F(\omega)/\omega$  using both Q and JT coupling; the dashed line is for  $\lambda_Q(\omega)$ , and the solid line is for  $\lambda_{JT}(\omega)$ . For  $\omega < 200 \text{ cm}^{-1}$  all contributions are from Q, whereas for  $\omega > 200 \text{ cm}^{-1}$  essentially all contributions are from JT. The maximum value of  $\lambda(\omega)$  is 0.0669 cm.

where  $W(\mathbf{q} + \mathbf{G}; \mathbf{k}', \mathbf{k}) = \sum_{m,n=1}^3 A_m^*(\mathbf{k}') A_n(\mathbf{k}) U_{mn}$  and  $U_{mn} = \sum_i e^{-i\mathbf{k}' \cdot \mathbf{R}_i} \langle \psi_m(\mathbf{R}_i) | e^{i(\mathbf{q} + \mathbf{G}) \cdot \mathbf{r}_i} | \psi_n(0) \rangle$ . Here  $\mathbf{q} = \mathbf{k}' - \mathbf{k} + \mathbf{G}$  is in the first Brillouin zone,  $\mathbf{G}$  is a reciprocal lattice vector,  $\mathbf{A}(\mathbf{k})$  is the electronic eigenvector of momentum  $\mathbf{k}$ ,  $\mathbf{R}_\alpha$  is the equilibrium position of the  $\alpha$ th atom in the unit cell,  $\psi_m$  is a local Wannier wave function, and  $\hat{V}_{ei}(\mathbf{q}) = 1/V_0 V_{ei}(\mathbf{q})$  ( $V_0$  is the volume of a unit cell).

All quantities in Eqs. 4–7 were obtained directly from first-principles calculations except the screening length,  $R_{sc}$ . From Thomas–Fermi theory (17–19) an estimate is  $R_{sc}^{TF} = \sqrt{E_f/6\pi e^2 n_e} = 0.63 \text{ \AA}$ , where  $n_e$  is the conduction electron density and  $E_f$  is the Fermi energy for free electron gas. The proper value of  $R_{sc}$  for  $\text{K}_3\text{C}_{60}$  should be somewhat larger, perhaps 0.7–1.2  $\text{\AA}$ .

To calculate  $\lambda_Q$ , we used three  $p$ -like Gaussian functions on each  $\text{C}_{60}$  to describe approximate Wannier  $t_{1u}$  orbitals from the three electronic bands. A typical function is  $\psi_x \propto x e^{-\alpha x^2 - \beta(y^2 + z^2)}$ , with  $\alpha = 0.0397 \text{ \AA}^{-2}$  and  $\beta = 0.0550 \text{ \AA}^{-2}$ . This treatment leads to analytic expressions for all integrals. We take the charge on each K as + electron and each C as  $-0.05$  electron.

As indicated in Fig. 1, we find that  $\lambda_Q(\omega)$  is negligible above  $200 \text{ cm}^{-1}$  and  $\lambda_Q$  has two peaks. One near  $\omega_Q \approx 20\text{--}40 \text{ cm}^{-1}$ , involves octahedral K plus  $\text{C}_{60}$  liberations; whereas the other at  $\omega_T \approx 130\text{--}150 \text{ cm}^{-1}$  involves tetrahedral K.

**Dynamic JT Coupling ( $H_{\text{ep}}^{\text{JT}}$ ).** Lannoo *et al.* (6, 7), Johnson *et al.* (8), and Varma *et al.* (9) suggested that JT coupling might play a role in the superconductivity, and Varma *et al.* (9) used modified neglect of differential overlap (MNDO) (20) calculations to estimate the couplings. We have repeated the estimates of Varma *et al.* (9) but using the vibrational modes from the GraFF (13) rather than from MNDO (20) (MNDO leads to frequencies  $\approx 11\%$  high). Letting  $g_m$  be the energy derivative with respect to displacement of  $m$  mode, we calculate (ref. 9 in parentheses): 0.19(0.1), 0.16(0.1), 0.26(0.2), 0.38(0.0), 0.26(0.6), 0.12(0.2), 1.77(1.8), and 1.49(1.2) for  $g_m$  of the eight  $H_g$  modes. This leads to (6–9)

$$\lambda_{JT,m} = \frac{5 N(0)}{6 M \omega_m^2} g_m^2, \quad [8]$$

shown in Fig. 1. Thus  $\lambda_{JT} = \sum_m \lambda_{JT,m} \sim \lambda_Q$  for  $R_{sc} \approx 0.6$  to  $1.0 \text{ \AA}$ .

### Calculations of $T_c$

**The Modified McMillan Equation.** McMillan (21) and then Allen and Dynes (22) succeeded in developing a general formula for how the transition temperature  $T_c$  depends on the phonon density of states and the electron–phonon coupling matrix. Starting with

$$\alpha_{\mathbf{k}}^2(\omega) F_{\mathbf{k}}(\omega) = \frac{1}{(2\pi)^3} \sum_j \int \frac{d^2\mathbf{k}}{v_F} |M_{\mathbf{k}'\mathbf{k}j}|^2 \delta(\omega - \Omega_{\mathbf{q}j})$$

$$\alpha^2(\omega) F(\omega) = \frac{1}{(2\pi)^3} \int \frac{d^2\mathbf{k}}{v_F} \alpha_{\mathbf{k}}^2(\omega) F_{\mathbf{k}}(\omega) \bigg/ \int \frac{d^2\mathbf{k}}{v_F} \quad [9]$$

$$\lambda = \int \lambda(\omega) d\omega = 2 \int \alpha^2(\omega) F(\omega) \frac{d\omega}{\omega}, \quad [10]$$

where  $v_F = \frac{1}{\hbar} \partial \epsilon_{\mathbf{k}} / \partial k_{\perp}$  is the average Fermi velocity ( $k_{\perp}$  is perpendicular to the Fermi surface), and  $\lambda$  is the coupling constant. They found that (21, 22)

$$T_c = \frac{\Theta}{1.20} \exp \left[ -\frac{1.04(1 + \lambda)}{\lambda - \mu^* - 0.62\lambda\mu^*} \right], \quad [11]$$

where various quantities are defined in Table 1.

### Results

Now defined are all quantities required to calculate the  $T_c$  from Eq. 11. Table 2 has the calculated superconducting

Table 1. Definitions of quantities in Eq. 11

$\Theta = f_1 f_2 \omega_{\log}$	$\mu^* = N(0) V_c / [1 + N(0) V_c \log(E_e / \omega_{\text{ph}})]$
$f_1 = \left[ 1 + \left( \frac{\lambda}{\Lambda_1} \right)^{3/2} \right]^{1/3}$	$f_2 = 1 + \frac{\left( \sqrt{\langle \omega^2 \rangle} / \omega_{\log} - 1 \right) \lambda^2}{\lambda^2 + \Lambda_2^2}$
$\Lambda_1 = 2.46 (1 + 3.8\mu^*)$	$\Lambda_2 = 1.82 (1 + 6.3\mu^*) \left( \sqrt{\langle \omega^2 \rangle} / \omega_{\log} \right)$
$\omega_{\log} = \exp \left[ \frac{2}{\lambda} \int_0^{\infty} \frac{d\omega}{\omega} \alpha^2(\omega) F(\omega) \log \omega \right]$	$\langle \omega^2 \rangle = \frac{2}{\lambda} \int_0^{\infty} d\omega \alpha^2(\omega) F(\omega) \omega$

$E_e$  and  $\omega_{\text{ph}}$  are the characteristic energy of conduction electron and phonon, respectively, and  $V_c = (4\pi e^2 / (k^2 + q_{sc}^2))$  is averaged over the Fermi surface. We take  $E_e = E_w = 0.6 \text{ eV}$  (the bandwidth) and  $\omega_{\text{ph}} = \omega_{\log}$ .

Table 2. Superconducting properties for different values of  $R_{sc}$  (the only variable in the calculations)

$R_{sc}$ (Å)	$\lambda_Q/\lambda_{JT}$	$\mu^*$	$\lambda$	$T_c$ (K)	$\Delta T_c$ (K) <sup>†</sup>	$\alpha_C$ <sup>‡</sup>	$\alpha_K$ <sup>‡</sup>
0.50	0.17	0.29	0.90	9.7	-6.4 (-3.6)	-0.10	-0.02
0.63	0.36	0.29	1.06	11.6	-8.7 (-5.8)	0.02	0.02
0.80	0.77	0.27	1.38	16.2	-9.9 (-5.3)	0.15	0.12
1.00	1.48	0.25	1.93	17.7	-5.8 (-0.5)	0.16	0.23
2.00	7.04	0.21	6.23	20.0	-0.1 (+3.2)	-0.01	0.44
Exp.				18 <sup>§</sup> , 19.3 <sup>¶</sup>	-7.2 <sup>  </sup>	0.30 (6) <sup>††</sup>	

Exp., experimental results.

<sup>†</sup>Change in  $T_c$  for pressure = 1 GPa = 10 kbar; in parentheses is the change assuming  $N(0) = 11.5$ .

<sup>‡</sup> $\alpha$  is the isotope exponent ( $T_c \propto M^{-\alpha}$ ).  $\alpha_C$  for  $^{12}\text{C} \rightarrow ^{13}\text{C}$  and  $\alpha_K$  for  $^{39}\text{K} \rightarrow ^{41}\text{K}$ .

<sup>§</sup>Ref. 1.

<sup>¶</sup>Ref. 3.

<sup>||</sup>Refs. 23–25.

<sup>††</sup>Ref. 26.

properties for various values of  $R_{sc}$ . These calculations use the density of states  $N(0) = 11.5$  from our tight-binding calculations. The susceptibility and critical field (23) suggest that  $N(0) \approx 10$ –15, whereas NMR measurement (24) gives  $N(0) \sim 20$ . An early photoemission experiment (25) reported that  $N(0) = 1.9$ , which may be low due to the surface sensitivity of these experiments.

We see that  $R_{sc} = 0.8$ –2.0 Å leads to  $T_c = 16$ –20 K, in good agreement with experiment (1–3). This does not prove the Q–JT mechanism because  $T_c$  depends sensitively upon  $N(0)$ , but neither experiment nor theory provides a precise value. The real test must be other properties.

Superconducting  $\text{K}_3\text{C}_{60}$  leads to an unusually large drop of  $T_c$  under external pressure (26),  $\Delta T_c \approx -7.2$  K for  $P = 1$  GPa. Using our force field, we calculated directly the equilibrium structure (allowing buckling of the buckyballs) and phonons for  $P = 1$  GPa and recalculated  $\lambda(\omega)$ . Here we used the LDA results (27) that  $N(0)$  decreases 20% under 1-GPa external pressure. The theory leads to  $\Delta T_c = -6$  to  $-10$  K for  $R_{sc} = 0.5$  to 1.0 Å.

A second significant test is the shift of  $T_c$  with isotope substitution. Experiments lead to  $\alpha_C = 0.30 \pm 0.06$  for  $\text{K}_3\text{C}_{60}$  (28) and  $\alpha_C = 0.37 \pm 0.05$  for  $\text{Rb}_3\text{C}_{60}$  (29) [an early report (30) of  $\alpha_C = 1.4 \pm 0.5$  may be inaccurate]. We recalculated all phonon states and  $\lambda(\omega)$  for both  $^{12}\text{C} \rightarrow ^{13}\text{C}$  and for  $^{39}\text{K} \rightarrow ^{41}\text{K}$ . The resulting  $\alpha_C = 0.15$  and 0.16 for  $R_{sc} = 0.8$  and 1.0 Å are in reasonable agreement with experiment (28–30), but  $R_{sc}$  outside this range would lead to  $\alpha_C$  in clear disagreement with experiment. A test here would be to measure  $\alpha_K$ , which we predict to be 0.12–0.23.

## Discussion

Our conclusion is that the superconductivity of  $\text{K}_3\text{C}_{60}$  is explained quite well by the Q–JT electron–phonon coupling mechanism including both  $H_{\text{ep}}^Q$  and  $H_{\text{ep}}^{\text{JT}}$  (with  $R_{sc} \approx 0.8$  to 1.0 Å). To test whether either  $H_{\text{ep}}^Q$  or  $H_{\text{ep}}^{\text{JT}}$  is sufficient, we carried out the same calculations using only one coupling.

Table 3. Effects of not having both Q coupling and JT coupling

$R_{sc}$ (Å)	Q coupling			JT coupling		
	$\delta T_c$ <sup>†</sup>	$\Delta T_c$ <sup>‡</sup>	$T_c$	$\delta T_c$ <sup>†</sup>	$\Delta T_c$ <sup>‡</sup>	$T_c$
0.50	NS	NS	NS	0.20	-0.73	1.52
0.63	0.00	NS	0.00	0.02	-0.01	0.02
0.80	0.00	-0.34	0.34	0.00	0.00	0.00
1.00	0.00	-2.26	2.50	0.00	0.00	0.00
2.00	0.00	-3.56	13.12	NS	NS	NS

All quantities are in the units of K. NS indicates not superconducting.

<sup>†</sup> $\delta T_c$  is the change for  $T_c$  upon  $^{12}\text{C} \rightarrow ^{13}\text{C}$ .

<sup>‡</sup> $\Delta T_c$  for 1 GPa pressure.

Table 3 shows that neither  $H_{\text{ep}}^Q$  nor  $H_{\text{ep}}^{\text{JT}}$  alone accounts for the superconducting properties of  $\text{K}_3\text{C}_{60}$ . With  $R_{sc} = 1.0$  Å,  $H_{\text{ep}}^Q$  leads to  $T_c = 2.5$  K, which drops for smaller  $R_{sc}$ . Larger values of  $R_{sc}$  with  $H_{\text{ep}}^Q$  alone lead to higher  $T_c$  values (e.g., 13 K for  $R_{sc} = 2.0$  Å) but  $\alpha_C \approx 0$ , in disagreement with experiment (28–30). Including only JT with  $R_{sc} = 0.5$  Å leads to  $T_c = 1.5$  K (which goes to zero for higher  $R_{sc}$ ) and a negative value of  $\alpha_C$ , also in disagreement with experiment (28–30); these results for JT alone differ from ref. 9 because they used a smaller, fixed value of  $\mu^*$ .

The conclusion here is that synergy between  $H_{\text{ep}}^Q$  and  $H_{\text{ep}}^{\text{JT}}$  leads to the special properties of buckyball superconductors. In the range  $R_{sc} = 0.8$ –1.0 Å,  $\lambda_Q/\lambda_{JT} \approx 0.8$ –1.5, so that both contributions are comparable. With only  $H_{\text{ep}}^Q$ ,  $T_c$  drops substantially because  $\lambda$  decreases and  $\omega_{\text{log}}$  becomes very small (decreasing  $\Theta$  of Eq. 11). For only JT,  $\lambda$  decreases, whereas  $\omega_{\text{log}}$  is very large, leading to a high  $\mu^*$  and, hence, a large negative exponential term in Eq. 11 and a low  $T_c$ .

The JT coupling essential to the Q–JT mechanism is large for  $\text{C}_{60}$  because of the high symmetry. Other buckyballs ( $\text{C}_{70}$ ,  $\text{C}_{76}$ ) have much lower symmetry and generally do not have a degenerate ground state (first-order JT coupling) for the anion. Because eliminating JT drops  $T_c$  from  $\sim 16$ –18 K to  $\sim 0$ –3 K, we expect other buckyballs to have  $T_c < 3$  K (potassium-intercalated graphite has  $T_c = 0.8$  K). We do not yet have a band structure for  $\text{Rb}_3\text{C}_{60}$  to fit to Eq. 3; however, we did a Q–JT calculation, assuming  $R_{sc} = 0.8$  Å, taking Fermi surface and  $\mu^*$  the same as  $\text{K}_3\text{C}_{60}$  and estimating  $N(0) = 1.2 \times 11.5$  [based on the result of an LDA calculation (27)]. Using the phonon states and optimal structure for  $\text{Rb}_3\text{C}_{60}$  from our force field (13) leads to  $T_c \approx 23.5$  K for  $\text{Rb}_3\text{C}_{60}$ , as compared with  $T_c = 16.2$  K for  $\text{K}_3\text{C}_{60}$  [experimental values (1–3) are 29 and 19 K, respectively].

Summarizing, we find that a combination of the charge and JT electron–phonon couplings are responsible for the superconductivity in  $\text{K}_3\text{C}_{60}$ . This explains  $T_c$ ,  $\Delta T_c$  (1 GPa), and  $\alpha_C$  (and predicts  $\alpha_K$ ). More definitive tests of this Q–JT mechanism will be the prediction of  $T_c$  for various mixed alkali systems (2–5) where  $T_c$  ranges from 2.5 to 33 K. There are no variables left to our disposal; thus the force fields (and hence phonons) are determined,  $R_{sc}$  must be  $\sim 0.8$ –1.0 Å, and the quantities in  $\mu^*$  are defined. The only remaining variables have to do with the electronic states [e.g.,  $N(0)$  and Fermi surface], which will emerge from LDA calculations.

We thank Drs. Y. Guo and N. Karasawa for discussions and help in calculating phonon eigenvectors and frequencies. This work was supported by National Science Foundation Grant CHE-91-00284 and by the Materials Simulation Center (California Institute of Technology) supported by Department of Energy (Advanced Industrial Concepts Division), Allied–Signal, Asahi Glass, Asahi Chemical, BP America, Chevron, and Xerox.

1. Hebard, A. F., Rosseinsky, M. J., Haddon, R. C., Murphy, D. W. & Glarum, S. H. (1991) *Nature (London)* **350**, 600–601.
2. Rosseinsky, M. J., Ramirez, A. P., Glarum, S. H., Murphy, D. W., Haddon, R. C., Hebard, A. F., Palstra, T. T. M., Kortan, A. R., Zahurak, S. M. & Makhija, A. V. (1991) *Phys. Rev. Lett.* **66**, 2830–2832.
3. Holczer, K., Klein, O., Huang, S.-M., Kaner, R. B., Fu, K.-J., Whetten, R. L. & Diederich, F. (1991) *Science* **252**, 1154–1157.
4. Tanigaki, K., Ebbesen, T. W., Saito, S., Mizuki, J., Tsai, J. S., Kubo, Y. & Kuroshima, S. (1991) *Nature (London)* **352**, 222–223.
5. Tanigaki, K., Hirose, I., Ebbesen, T. W., Mizuki, J., Shimakawa, Y., Kubo, Y., Tsai, J. S. & Kuroshima, S. (1991) *Nature (London)* **356**, 419–421.
6. Lannoo, M., Baraff, G. A., Schluter, M. & Tomanek, D. (1991) *Phys. Rev. B* **44**, 12106–12108.
7. Schluter, M., Lannoo, M., Needels, M., Baraff, G. A. & Tomanek, D. (1992) *Phys. Rev. Lett.* **68**, 526–529.
8. Johnson, K. H., McHenry, M. E. & Clougherty, D. P. (1991) *Physica C* **183**, 319–323.
9. Varma, C. M., Zaanen, J. & Raghavachari, K. (1991) *Science* **254**, 989–992.
10. Zhang, F. C., Ogata, M. & Rice, T. M. (1991) *Phys. Rev. Lett.* **67**, 3452–3455.
11. Chakravarty, S., Gelfand, M. P. & Kivelson, S. (1991) *Science* **254**, 970–974.
12. Baskaran, G. & Tosatti, E. (1991) *Curr. Sci. (India)* **61**, 33–39.
13. Guo, Y., Karasawa, N. & Goddard, W. A., III (1991) *Nature (London)* **351**, 464–467.
14. Stephens, P. W., Mihaly, L., Lee, P. L., Whetten, R. L. & Huang, S. M. (1991) *Nature (London)* **351**, 632–634.
15. Zhou, O., Vaughan, G. B. M., Zhu, Q., Fisher, J. E., Heiney, P. A., Coustel, N., McCauley, J. P. & Smith, A. B., III (1992) *Science* **255**, 833–835.
16. Erwin, S. C. & Pickett, W. E. (1991) *Science* **254**, 842–845.
17. Fermi, E. (1928) *Z. Phys.* **48**, 73–79.
18. Thomas, L. H. (1927) *Proc. Cambridge Philos. Soc.* **23**, 542–548.
19. Mahan, G. D. (1981) *Many-Particle Physics* (Plenum, New York), pp. 420–422.
20. Dewar, M. J. S. & Thiel, W. (1977) *J. Am. Chem. Soc.* **99**, 4899–4917.
21. McMillan, W. L. (1968) *Phys. Rev.* **167**, 331–344.
22. Allen, P. B. & Dynes, R. C. (1975) *Phys. Rev. B* **12**, 905–922.
23. Ramirez, A. P., Rosseinsky, M. J., Murphy, D. W., Fleming, R. M. & Haddon, R. C. (1992) *Bull. Am. Phys. Soc.* **37**, 714 (abstr.).
24. Tycko, R., Dabbagh, G., Rosseinsky, M. J., Murphy, D. W. & Fleming, R. M. (1991) *Science* **253**, 884–886.
25. Chen, C. T., Tjeng, L. H., Rodolf, P., Meigs, G., Rowe, J. E., Chen, J., McCauley, J. P., Smith, A. B., McGhie, A. R., Romanow, W. J. & Plummer, E. W. (1991) *Nature (London)* **352**, 603–605.
26. Sparn, G., Thompson, J. D., Huang, S.-M., Kaner, R. B., Diederich, F., Whetten, R. L., Gruner, G. & Holczer, K. (1991) *Science* **252**, 1829–1831.
27. Oshiyama, A. & Saito, S. (1992) *Solid State Commun.* **82**, 41–45.
28. Chen, C.-C. & Lieber, C. M. (1992) *J. Am. Chem. Soc.* **114**, 3141–3142.
29. Ramirez, A. P., Kortan, A. R., Rosseinsky, M. J., Duclos, S. J., Mujsce, A. M., Haddon, R. C., Murphy, D. W., Makhija, A. V., Zahurak, S. M. & Lynos, K. B. (1992) *Phys. Rev. Lett.* **68**, 1058–1060.
30. Ebbesen, T. W., Tsai, J. S., Tanigaki, K., Tabuchi, J. & Shimakawa, Y. (1992) *Nature (London)* **355**, 620–622.